Prostaglandin E_2 down-regulates sirtuin 1 (SIRT1), leading to elevated levels of aromatase, providing insights into the obesity–breast cancer connection

Received for publication, September 14, 2018, and in revised form, November 5, 2018 Published, Papers in Press, November 8, 2018, DOI 10.1074/jbc.RA118.005866

Kotha Subbaramaiah[‡1], Neil M. Iyengar[§], Monica Morrow[¶], Olivier Elemento[‖], Xi Kathy Zhou[‡‡], and Andrew J. Dannenberg[‡2]**

*From the Departments of [‡]Medicine and [‖]Physiology and Biophysics, the **Caryl and Israel Englander Institute for Precision Medicine, and the [‡‡]Healthcare Policy and Research, Weill Cornell Medical College, New York, New York 10065 and the Departments of [§]Medicine and [¶]Surgery, Memorial Sloan Kettering Cancer Center, New York, New York 10065*

Edited by Xiao-Fan Wang

Obesity increases the risk of hormone receptor–positive breast cancer in postmenopausal women. Levels of aromatase, the rate-limiting enzyme in estrogen biosynthesis, are increased in the breast tissue of obese women. Both prostaglandin E_2 (PGE_2) and hypoxia-inducible factor 1α (HIF-1α) contribute to the induction of aromatase in adipose stromal cells (ASCs). Sirtuin 1 (SIRT1) binds, deacetylates, and thereby inactivates HIF-1α. Here, we sought to determine whether SIRT1 also plays a role in regulating aromatase expression. We demonstrate that reduced SIRT1 levels are associated with elevated levels of acetyl–HIF-1α, HIF-1α, and aromatase in breast tissue of obese compared with lean women. To determine whether these changes were functionally linked, ASCs were utilized. In ASCs, treatment with PGE_2, which is increased in obese individuals, down-regulated SIRT1 levels, leading to elevated acetyl–HIF-1α and HIF-1α levels and enhanced aromatase gene transcription. Chemical SIRT1 activators (SIRT1720 and resveratrol) suppressed the PGE_2-mediated induction of acetyl–HIF-1α, HIF-1α, and aromatase. Silencing of p300/CBP-associated factor (PCAF), which acetylates HIF-1α, blocked PGE_2-mediated increases in acetyl–HIF-1α, HIF-1α, and aromatase. SIRT1 overexpression or PCAF silencing inhibited the interaction between HIF-1α and p300, a coactivator of aromatase expression, and suppressed p300 binding to the aromatase promoter. PGE_2 acted via prostaglandin E2 receptor 2 (EP_2) and EP_4 to induce activating transcription factor 3 (ATF3), a repressive transcription factor, which bound to a CREB site within the *SIRT1* promoter and reduced SIRT1 levels. These findings suggest that reduced SIRT1-mediated deacetylation of HIF-1α contributes to the elevated levels of aromatase in breast tissues of obese women.

Obesity is a risk factor for the development of estrogen receptor-positive (ER+)[3] breast cancer in postmenopausal women (1–3). In addition to its impact on breast cancer risk, obesity is recognized to be a poor prognostic factor for patients with ER+ breast cancer (4–8). Cytochrome P450 aromatase, a product of the *CYP19A1* gene, is the rate-limiting enzyme for the synthesis of estrogens from androgens (9). Increased levels of aromatase are found in the breast tissue of obese women, which helps to explain the link between obesity and ER+ breast cancer (10, 11). It is important, therefore, to elucidate the mechanisms that lead to elevated aromatase expression in the breast tissue of obese women. The expression of aromatase is tightly regulated, with its transcription controlled by several tissue-specific promoters. In normal breast adipose, aromatase is under the control of promoter I.4 and expressed at low levels. By contrast, in obesity, the coordinated activation of promoters I.3 and II leads to a significant increase in aromatase expression (11). The proximal promoters I.3 and II are located near each other, stimulated by activation of the cAMP → PKA → cAMP-response element–binding protein (CREB) pathway, and aided by many other regulators, including hypoxia inducible factor-1α (HIF-1α). Prostaglandin E_2 (PGE_2), a bioactive lipid that is elevated in obesity, can induce HIF-1α, contributing, in turn, to enhanced *CYP19A1* transcription in adipose stromal cells (ASCs) (11–13). These cells are believed to be a major source of estrogen that acts in a paracrine manner to stimulate tumor formation and growth (12, 14, 15). Although HIF-1α plays a critical role in regulating aromatase expression in breast ASCs, the mechanisms that control HIF-1α activity are incompletely understood.

HIF-1α and HIF-1β heterodimerize to form HIF-1, which binds to core hypoxia response elements and induces the expression of genes responsible for metabolic reprogramming, angiogenesis, and metastasis (16–18). The activity of HIF-1 is primarily regulated by oxygen-dependent protein degradation and the transactivation function of HIF-1α. Under normoxic

This work was supported, in whole or part, by National Institutes of Health Grants R01CA215797 and U54 CA210184, the Breast Cancer Research Foundation, and the Botwinick-Wolfensohn Foundation (in memory of Mr. and Mrs. Benjamin Botwinick). The authors declare that they have no conflicts of interest with the contents of this article. The content is solely the responsibility of the authors and does not necessarily represent the official views of the National Institutes of Health.

This article contains Fig. S1.

[1] To whom correspondence may be addressed: Weill Cornell Medical College, 525 E. 68th St., Rm. E-803, New York, NY 10065. Tel.: 646-962-2892; Fax: 646-962-0891; E-mail: ajdannen@med.cornell.edu.

[2] To whom correspondence may be addressed: Weill Cornell Medical College, 525 E. 68th St., Rm. E-803, New York, NY 10065. Tel.: 646-962-2893; Fax: 646-962-0891; E-mail: ksubba@med.cornell.edu.

[3] The abbreviations used are: ER, estrogen receptor; CRE, cyclic AMP-response element; CREB, CRE–binding protein; HIF-1α, hypoxia inducible factor-1α; PGE_2, prostaglandin E_2; ASC, adipose stromal cell; SIRT1, sirtuin 1; BMI, body mass index; PCAF, p300/CBP-associated factor; PKA, protein kinase A; ATF3, activating transcription factor 3; EP, prostaglandin E2 receptor; HRE, hypoxia-responsive element; FPKM, fragments per kilobase per million.

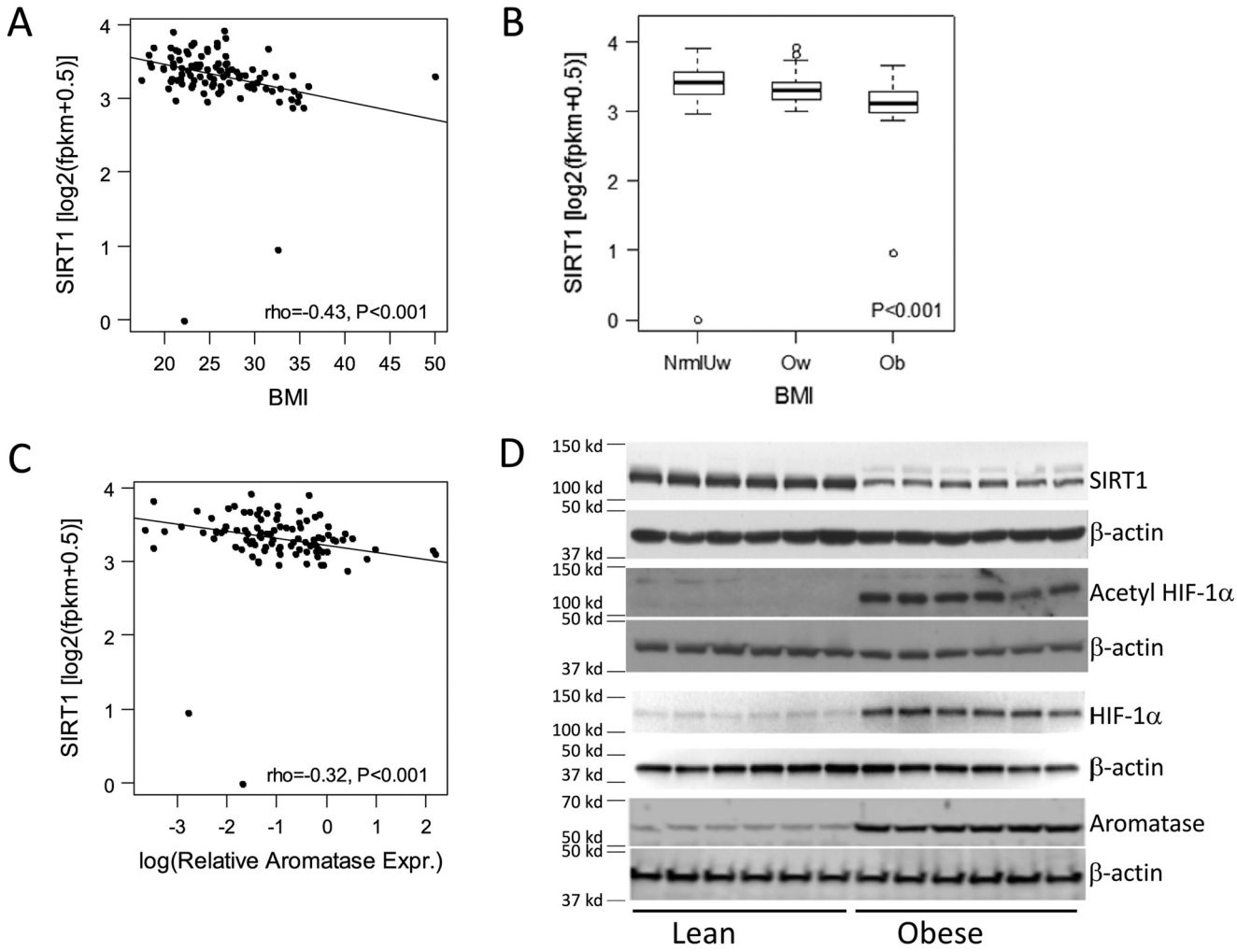

Figure 1. Elevated BMI is associated with decreased expression of SIRT1 and increased acetyl–HIF-1α, HIF-1α, and aromatase in the breast. *A*, higher BMI correlates with decreased SIRT1 mRNA levels in breast tissue. *B*, obese women have decreased levels of SIRT1 mRNA in the breast compared with overweight or lean women (normal/underweight, $n = 48$; overweight, $n = 33$; obese, $n = 19$). *Error bars*, S.D. *C*, levels of SIRT1 and aromatase mRNAs are inversely correlated. RNA-Seq was used to quantify SIRT1 levels in *A–C*. *D*, immunoprecipitation followed by Western blotting demonstrated decreased levels of SIRT1 and increased levels of acetyl–HIF-1α, HIF-1α, and aromatase in breast tissue of obese ($n = 6$) *versus* lean ($n = 6$) women.

conditions, HIF-1α is hydroxylated, which triggers ubiquitination leading to rapid proteolysis. By contrast, under hypoxic conditions, HIF-1α becomes stable and active because of inactivation of oxygen-dependent hydroxylases. The longevity-associated protein sirtuin 1 (SIRT1) has protein deacetylase activity and targets many transcription factors, including HIF-1α (19–21). SIRT1 binds to HIF-1α and deacetylates it, thereby inactivating HIF-1α (22). Levels of SIRT1 are reduced in the adipose tissue of obese humans (23–26). Collectively, these findings suggest the possibility that the increased expression of aromatase found in the breast tissue of obese women could be due, in part, to reduced expression of SIRT1, resulting in elevated levels of acetylated HIF-1α and activation of *CYP19A1* gene expression.

In the present study, we had two main objectives. The first was to determine whether SIRT1 levels were reduced in breast tissue from obese *versus* lean women and correlated with levels of acetylated HIF-1α, HIF-1α, and aromatase. A second goal was to elucidate the role of SIRT1 in PGE_2-mediated induction of aromatase. We present evidence that SIRT1 levels are reduced in the breast tissue of obese women and inversely correlated with levels of acetylated HIF-1α, HIF-1α, and aromatase. Moreover, new insights are provided into the signaling pathway by which PGE_2 inhibits *SIRT1* gene expression, leading, in turn, to increased levels of acetylated HIF-1α and aromatase in ASCs.

Results

Levels of SIRT1 are decreased in the breast tissue of obese women and correlate with amounts of acetyl–HIF-1α, HIF-1α, and aromatase

Initially, we correlated breast levels of SIRT1 mRNA with body mass index (BMI). SIRT1 mRNA levels negatively correlated with BMI (Fig. 1*A*) and were lowest in the breast tissue of obese women (Fig. 1*B*). To determine whether there was a potential relationship between SIRT1 and aromatase, levels of these two mRNAs were correlated. As shown in Fig. 1*C*, a negative correlation was found between levels of SIRT1 and aromatase mRNAs. Because SIRT1 can deacetylate and inactivate HIF-1α, a known regulator of *CYP19A1* transcription, we also compared levels of SIRT1, acetyl–HIF-1α, HIF-1α, and aroma-

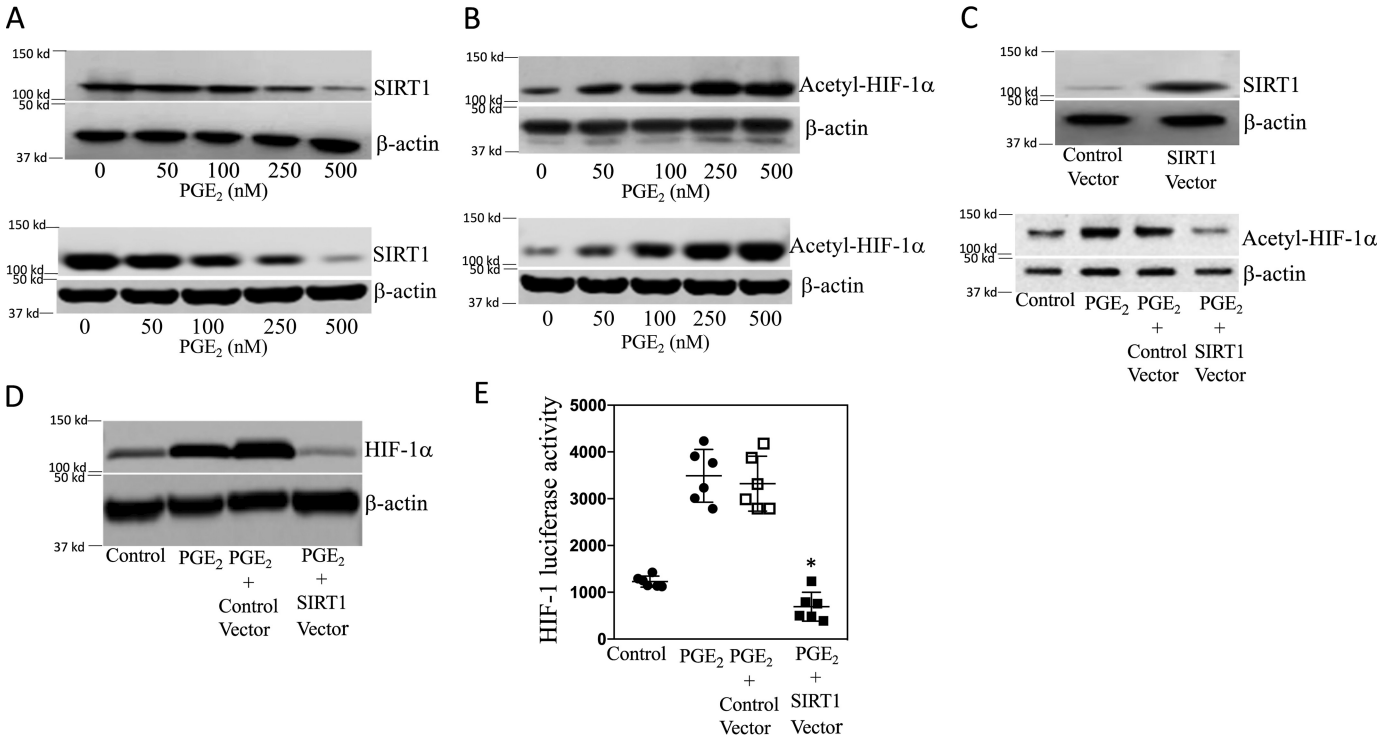

Figure 2. PGE_2 increases HIF-1 activity by suppressing SIRT1 levels in human breast adipose stromal cells. *A–E*, human breast ASC cell line was used. *A* and *B*, the *bottom panels* represent primary human breast ASCs. *A* and *B*, cells were treated with the indicated concentrations of PGE_2 for 24 h. Cells were then harvested, and lysates were subjected to Western blotting. *C* and *D*, cells were transfected with 2 μg of control vector or SIRT1 expression vector as indicated. *C* (*top*), cells were harvested, and Western blotting was performed for SIRT1 and β-actin to confirm overexpression. *C* (*bottom*) and *D*, cells were treated with vehicle or 500 nM PGE_2 for 24 h. Cell lysates were prepared and subjected to Western blotting, and the blots were probed as indicated. *E*, cells were transfected as indicated with 0.9 μg of HRE-luciferase and 0.2 μg of *psv*β-gal constructs. Cells labeled *Control Vector* also received 0.9 μg of expression vector; cells labeled *SIRT1 Vector* also received 0.9 μg of SIRT1 expression vector. 24 h after transfection, cells were treated with vehicle (control) or 500 nM PGE_2 for 24 h. Cells were harvested, and luciferase activity was measured. Luciferase activity was normalized to β-gal activity. Means ± S.D. (*error bars*) are shown, $n = 6$. *, $p < 0.001$ *versus* PGE_2-treated cells expressing control vector.

tase proteins in the breast tissue of obese *versus* lean women. Following immunoprecipitation, Western blotting was performed and revealed reduced levels of SIRT1 in association with higher levels of acetylated HIF-1α, HIF-1α, and aromatase in breast tissue from obese *versus* lean women (Fig. 1*D*).

PGE_2-mediated induction of aromatase depends on acetylation of HIF-1α

Although HIF-1α is important for PGE_2-mediated induction of aromatase (12), the role of SIRT1 has not been investigated. We determined the effects of PGE_2 on SIRT1 levels. Treatment of breast ASCs with PGE_2 led to a dose-dependent decrease in SIRT1 protein levels (Fig. 2*A*). Because HIF-1α can be deacetylated by SIRT1, we measured levels of acetyl–HIF-1α following treatment with PGE_2. Levels of acetyl–HIF-1α increased in response to PGE_2 treatment and were inversely related to the levels of SIRT1 in both immortalized human breast ASCs (*top panel* in Fig. 2, *A* and *B*) and primary human breast ASCs (*bottom panel* in Fig. 2, *A* and *B*). To confirm the importance of SIRT1 in regulating levels of acetyl–HIF-1α, we next overexpressed SIRT1. As shown in Fig. 2*C*, the increase in acetyl–HIF-1α levels mediated by PGE_2 was suppressed by overexpressing SIRT1. Similar changes in levels of HIF-1α were observed (Fig. 2*D*). To determine the functional consequences of PGE_2-mediated induction of acetyl–HIF-1α, transient transfections were performed utilizing an HRE-*luc* reporter construct. Treatment with PGE_2 stimulated HIF-1 activity, an effect that was abrogated by overexpressing SIRT1 (Fig. 2*E*). Because HIF-1α plays a role in PGE_2-mediated induction of aromatase, we next evaluated levels of SIRT1 and aromatase over time following treatment with PGE_2. Treatment with PGE_2 led to a time-dependent decline in SIRT1 levels in association with a reciprocal increase in aromatase protein and acetyl–HIF-1α levels (Fig. 3, *A* and *B*). To determine whether the reduced levels of SIRT1 mediated by PGE_2 were causally linked to the increase in aromatase, we overexpressed SIRT1 in ASCs. Overexpressing SIRT1 blocked PGE_2-mediated induction of aromatase protein and mRNA (Fig. 3, *C–E*). To determine whether overexpressing SIRT1 altered aromatase transcription, transient transfections were performed. Overexpressing SIRT1 blocked PGE_2-mediated stimulation of aromatase promoter activity (Fig. 3*F*). To investigate whether SIRT1 altered the binding of HIF-1α to the *CYP19A1* promoter in response to PGE_2, ChIP assays were performed. ChIP assays revealed increased binding of HIF-1α to the *CYP19A1* promoter, an effect that was abrogated by overexpressing SIRT1 (Fig. 3*G*). To complement these studies, we also utilized small molecules that activate SIRT1. Consistent with the effects of overexpressing SIRT1, activators of SIRT1 (SIRT1720 and resveratrol) blocked PGE_2-mediated induction of acetyl–HIF-1α, HIF-1α, and aromatase (Fig. 4).

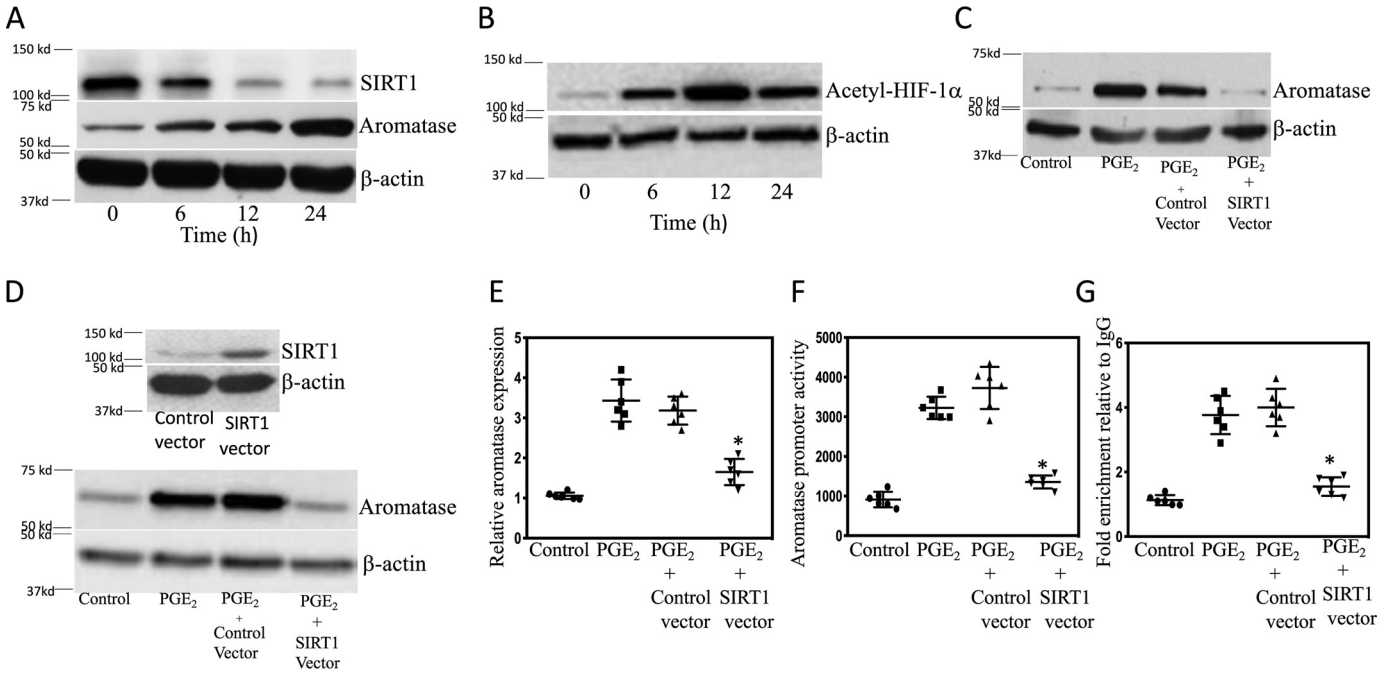

Figure 3. Overexpression of SIRT1 inhibits PGE_2-mediated induction of aromatase. Human breast ASC cell line was used except in *D*, where primary human breast ASCs were employed. *A* and *B*, cells were treated with 500 nM PGE_2 for 0–24 h as indicated. *C–E*, cells were either untransfected (*Control*) or transfected as indicated. Cells were then treated with vehicle or 500 nM PGE_2 for 24 h. *A–D*, cell lysates were subjected to Western blotting, and the blots were probed as indicated. *E*, aromatase mRNA levels were determined by quantitative PCR. *F*, cells were transfected with 0.9 μg of aromatase promoter PII-luciferase and 0.2 μg of *psvβ*-gal constructs. In addition, as indicated, cells received 0.9 μg of control expression vector or SIRT1 expression vector. Cells were treated with vehicle (control) or 500 nM PGE_2 for 24 h. Cells were harvested, and luciferase activity was measured. Luciferase activity was normalized to β-gal activity. *G*, cells were either untransfected or transfected with 0.9 μg of control vector or SIRT1 expression vector. Subsequently, cells were treated with vehicle or 500 nM PGE_2 for 3 h. ChIP assays were performed. Chromatin fragments were immunoprecipitated with antibodies against HIF-1α, and the aromatase promoter was amplified by real-time PCR. DNA sequencing was carried out, and the PCR products were confirmed to be the aromatase promoter. This promoter was not detected when normal IgG was used or when antibody was omitted from the immunoprecipitation step. In *E–G*, means ± S.D. (*error bars*) are shown ($n = 6$). *, $p < 0.001$.

Because p300/CBP-associated factor (PCAF) can acetylate and activate HIF-1α (22), we next investigated whether silencing PCAF would attenuate PGE_2-mediated induction of aromatase. First we showed that silencing PCAF led to a reduction in acetyl–HIF-1α (Fig. 5*A*). Moreover, the increase in levels of acetyl–HIF-1α and HIF-1α mediated by PGE_2 was blocked by silencing PCAF (Fig. 5, *B* and *C*). Silencing PCAF also blocked the induction of aromatase by PGE_2 (Fig. 5*D*). Acetylation of HIF-1α has been shown to enhance its interaction with p300 (22), a coactivator that plays a role in regulating aromatase expression (27). Next, we examined the role of acetylation of HIF-1α in its interaction with p300 in response to PGE_2. As shown in Fig. 6 (*A* and *B*), treatment of cells with PGE_2 increased the interaction of HIF-1α with p300, an effect that was abrogated when either SIRT1 was overexpressed or PCAF was silenced. Subsequently, ChIP assays were performed to determine the effects of overexpressing SIRT1 or silencing PCAF on PGE_2-mediated induction of p300 binding to the *CYP19A1* promoter. As shown in Fig. 6 (*C* and *D*), the increase in binding of p300 to the *CYP19A1* promoter mediated by PGE_2 was abrogated by overexpressing SIRT1 or silencing PCAF.

PGE_2 suppresses SIRT1 transcription via EP_2 and EP_4

Having demonstrated that PGE_2 down-regulated SIRT1 protein levels (Fig. 2*A*), we next explored the underlying mechanism. Treatment with PGE_2 caused dose-dependent suppression of SIRT1 mRNA levels (Fig. 7*A*). Transient transfections were performed to determine the effect of PGE_2 on *SIRT1* promoter activity. As shown in Fig. 7*B*, treatment with PGE_2 reduced *SIRT1* promoter activity. PGE_2 mediates its effects by binding to EP receptors. A combination of EP receptor agonists and antagonists was used to determine which EP receptors were responsible for PGE_2-mediated suppression of *SIRT1* transcription. Both butaprost, an EP_2 receptor agonist, and CAY10684, an EP_4 receptor agonist, down-regulated SIRT1 (Fig. 7, *C* and *D*). Moreover, PGE_2-mediated down-regulation of SIRT1 was prevented by treatment with EP_2 (PF04418948) and EP_4 (ONO AE3 208) receptor antagonists (Fig. 7, *E* and *F*). Binding of PGE_2 to EP_2 or EP_4 receptors can stimulate protein kinase A (PKA) activity. Hence, we next determined whether PKA was involved in reducing SIRT1 levels in response to PGE_2. Treatment with H89, a PKA inhibitor, prevented the decrease in SIRT1 levels mediated by PGE_2 (Fig. 8*A*). PGE_2 also induced ATF3 in both immortalized human breast ASCs and primary human breast ASCs (Fig. 8*B* and Fig. S1*A*). Treatment with either an EP_2 or EP_4 receptor agonist also induced ATF3 (Fig. S1, *B* and *C*). Inhibition of PKA with H89 blocked PGE_2-mediated induction of ATF3 (Fig. 8*C*). To determine whether this increase in ATF3 was important for explaining the reduction in SIRT1 levels, transient transfections were performed. Interestingly, PGE_2-mediated suppression of *SIRT1* promoter activity was relieved by silencing ATF3 (Fig. 8*D*). Next, we attempted to localize the site in the *SIRT1* promoter that was

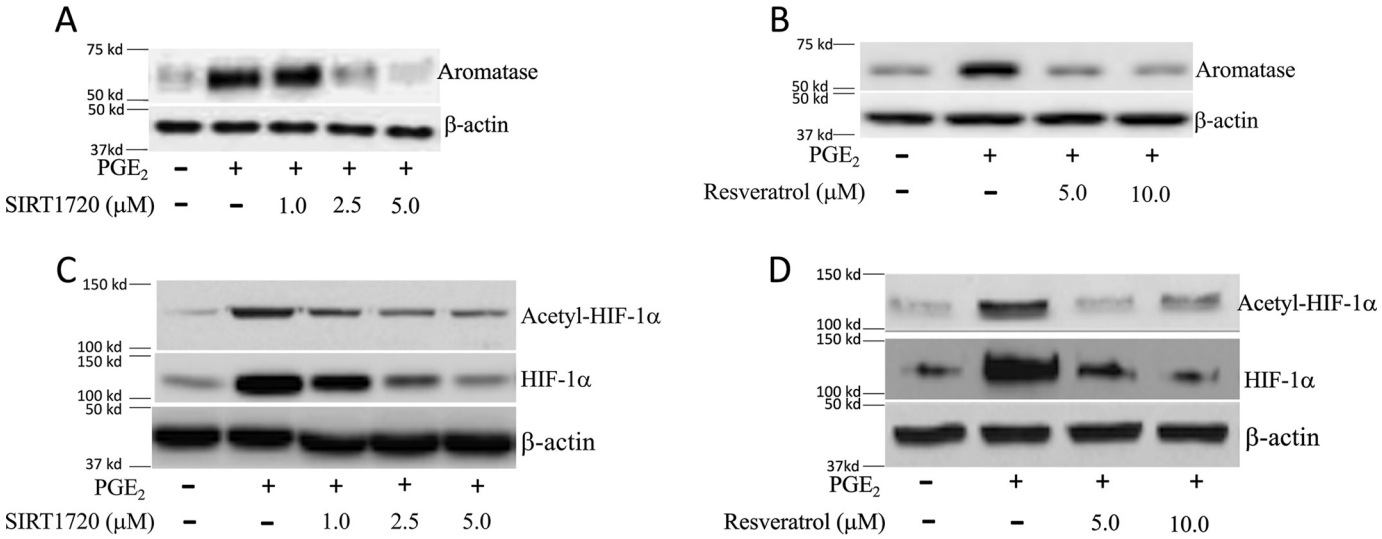

Figure 4. SIRT1 activators inhibit PGE_2-mediated induction of acetyl–HIF-1α, HIF-1α and aromatase. The human breast ASC cell line was used. Cells were treated with vehicle, 500 nM PGE_2, or PGE_2 plus the indicated concentrations of SIRT1720 (*A* and *C*) or resveratrol (*B* and *D*) for 24 h. Cell lysates were subjected to Western blotting as indicated.

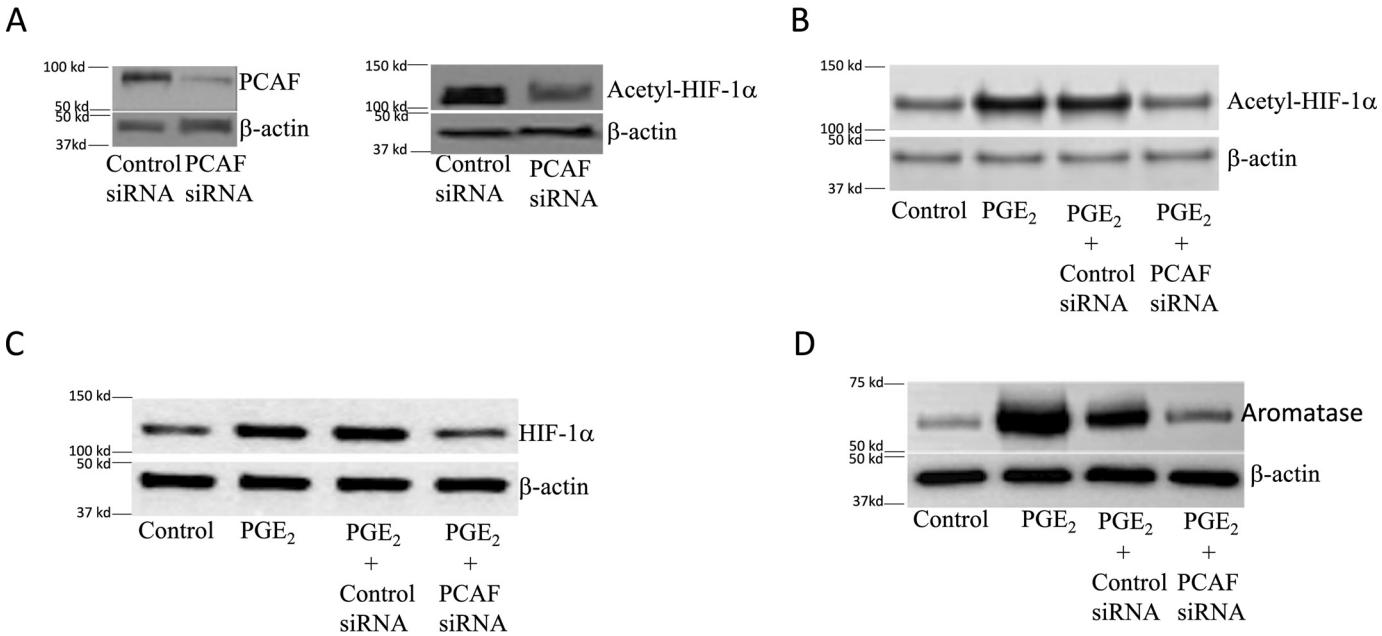

Figure 5. Silencing PCAF inhibits PGE_2-mediated induction of aromatase. *A–D*, human breast ASC cell line was used. Cells were either untransfected or transfected as indicated with 2 μg of siRNA to GFP (control siRNA) or PCAF siRNA. *A*, 48 h after transfection, cells were harvested, and Western blotting was performed for PCAF, acetyl–HIF-1α, and β-actin. *B–D*, cells were treated with vehicle (control) or 500 nM PGE_2 for 24 h. Cell lysates were subjected to Western blotting, and the blots were probed as indicated.

responsible for mediating the suppressive effects of PGE_2. Transient transfections were carried out utilizing a series of *SIRT1* promoter deletion constructs (Fig. 8*E*). The suppressive effects of PGE_2 were lost when promoter deletion construct 2 (Del2) that lacks the CRE site was used. ChIP assays were performed to determine whether ATF3 bound to the *SIRT1* promoter in response to treatment with PGE_2. In fact, PGE_2 stimulated the binding of ATF3 to the *SIRT1* promoter (Fig. 8*F*). Finally, we determined whether silencing ATF3 would block PGE_2-mediated induction of aromatase. As shown in Fig. 8*G*, silencing ATF3 suppressed PGE_2-mediated induction of aromatase. Taken together, these data suggest that PGE_2 binds to EP_2 and EP_4 receptors, leading to down-regulation of SIRT1, enhanced acetylation of HIF-1α, and increased aromatase expression in ASCs.

Discussion

The current study provides new insights into the mechanisms that underlie the elevation of aromatase expression in the breast tissue of obese women. Mechanistic studies were carried out in ASCs because obesity is associated with increased levels of both HIF-1α and aromatase in these cells (28). We focused on SIRT1 because of evidence that it can deacetylate and inactivate HIF-1α, raising the possibility that SIRT1 could modulate *CYP19A1* gene expression and thereby aromatase levels (22).

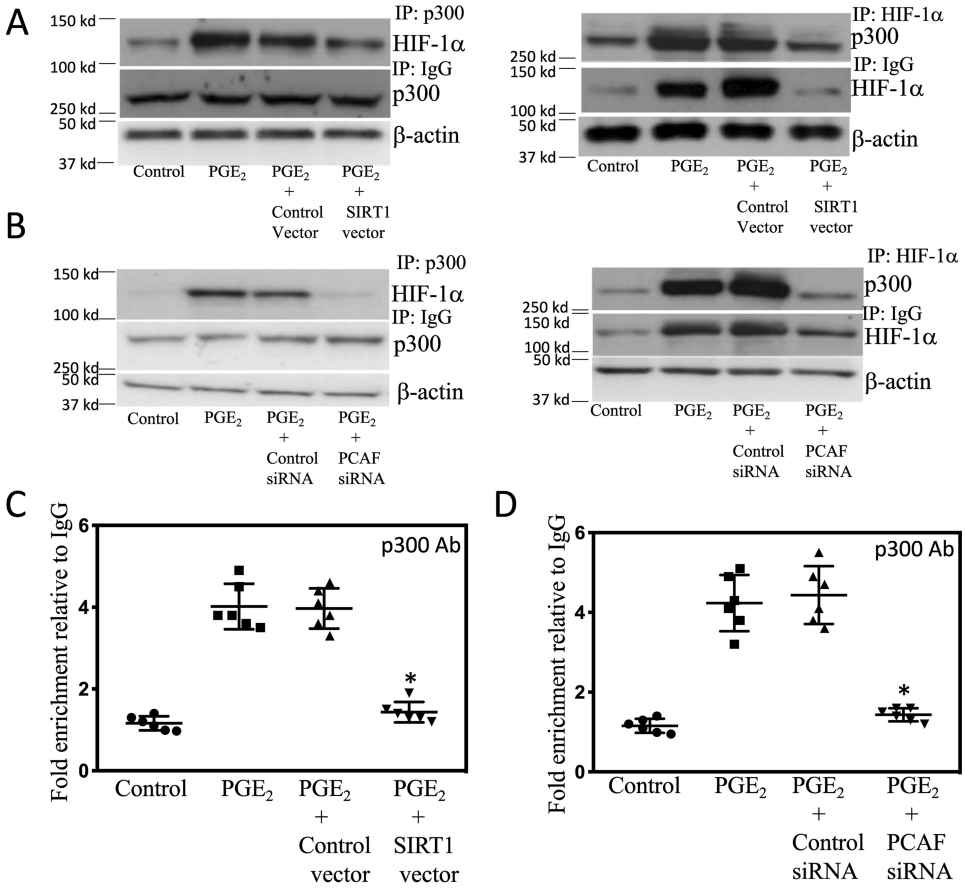

Figure 6. SIRT1 and PCAF regulate the binding of p300 to the *CYP19A1* promoter. *A–D*, human breast ASC cell line was used. *A*, cells were either untransfected or transfected with 2 μg of control vector or SIRT1 expression vector for 48 h. Cells were then treated with vehicle (control) or 500 nM PGE_2 for 3 h. *B*, cells were either untransfected or transfected with 2 μg of siRNA to GFP (control siRNA) or PCAF siRNA for 48 h. Cells were then treated with vehicle (control) or 500 nM PGE_2 for 3 h. *A* and *B*, cell lysates were subjected to immunoprecipitation (*IP*) with p300 (*left*) or HIF-1α (*right*) antisera or IgG, and immunoprecipitates were subjected to Western blotting and probed as indicated. *C* and *D*, ChIP assays were performed. *C*, cells were either untransfected or transfected with 2 μg of control vector or SIRT1 expression vector for 48 h. *D*, cells were either untransfected or transfected with 2 μg of siRNA to GFP (control siRNA) or PCAF siRNA for 48 h. *C* and *D*, cells were then treated as indicated with vehicle (control) or 500 nM PGE_2 for 3 h. Chromatin fragments were immunoprecipitated with antibodies against p300, and the aromatase promoter was amplified by real-time PCR. DNA sequencing was carried out, and the PCR products were confirmed to be the aromatase promoter. This promoter was not detected when normal IgG was used or when antibody was omitted from the immunoprecipitation step. In *C* and *D*, means ± S.D. (*error bars*) are shown ($n = 6$). *, $p < 0.001$.

Several lines of evidence suggest the importance of SIRT1 and the acetylation of HIF-1α as determinants of aromatase expression in the breast tissue of obese women. Reduced levels of SIRT1 correlated with increased levels of acetylated HIF-1α, HIF-1α, and aromatase in the breast tissue of obese *versus* lean women. Notably, the reduction in SIRT1 mRNA and protein in the breast tissue of obese women is consistent with prior evidence that SIRT1 levels are decreased in adipose tissue of obese humans (23–26). The reduction in SIRT1 levels has been attributed to hypoxia and an associated decrease in NAD^+ levels (23). Saturated fatty acids and reactive oxygen species have also been suggested to play a role in down-regulating SIRT1 (23). We focused on PGE_2 because levels of this bioactive lipid are increased in the breast tissue of obese women, and it is a known inducer of HIF-1α and aromatase in ASCs (11, 12, 28). More specifically, PGE_2 is known to increase HIF-1α transcript and protein expression and binding to *CYP19A1* promoter II, leading to increased aromatase levels. Here, we found that PGE_2-mediated suppression of SIRT1 levels was associated with elevated levels of acetylated HIF-1α, HIF-1α, HIF-1 activity, and aromatase. Importantly, these inductive effects of PGE_2, including the activation of *CYP19A1* transcription, were abrogated by overexpressing SIRT1 or treatment with two activators of SIRT1 (SIRT1720 and resveratrol). Taken together, these results underscore the importance of acetylated HIF-1α as a determinant of aromatase expression.

The coactivator CBP/p300 possesses histone acetyltransferase activity and plays an important role in stabilizing HIF-1α protein and mediating the induction of aromatase in response to PGE_2 treatment (27, 29). The acetylation status of HIF-1α is a determinant of its ability to bind to p300 and thereby regulate gene expression (22, 29). PCAF acetylates HIF-1α, whereas SIRT1 deacetylates it at Lys-674 (22). Thus, HIF-1α activity, including its ability to interact with p300, appears to be balanced by the opposing activities of PCAF and SIRT1. In the present study, we show for the first time that PCAF is important for PGE_2-mediated induction of aromatase. Silencing PCAF suppressed PGE_2-mediated induction of acetyl–HIF-1α, HIF-1α, and aromatase. PGE_2 treatment led to enhanced interaction between p300 and HIF-1α, an effect that was reduced when either SIRT1 was overexpressed or PCAF was silenced. Moreover, overexpression of SIRT1 or silencing PCAF blocked

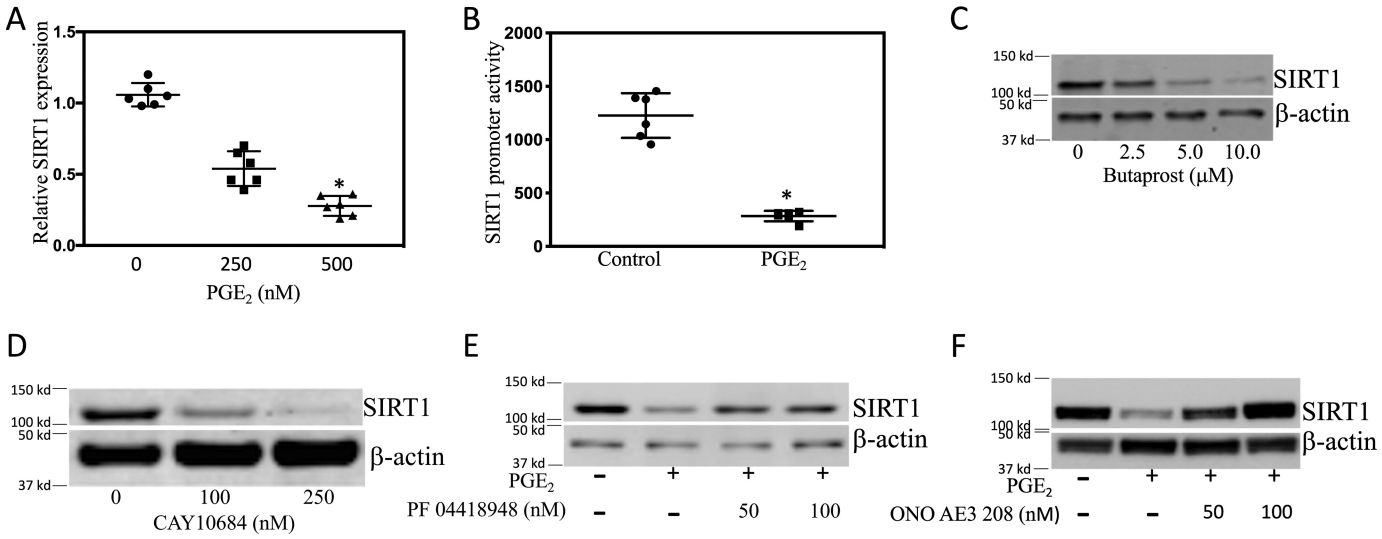

Figure 7. PGE_2 down-regulates SIRT1 expression in human breast ASCs. *A*, cells were treated with the indicated concentrations of PGE_2 for 24 h. Total RNA was isolated, and quantitative PCR for SIRT1 was performed. *B*, cells were transfected with 1.8 μg of full-length *SIRT1* promoter and 0.2 μg of *psv*-β-gal constructs. 24 h after transfection, cells were treated with vehicle or 500 nM PGE_2 for 24 h. Cells were harvested, and luciferase activity was measured. Luciferase activity was normalized to β-gal activity. *C* and *D*, cells were treated with vehicle (control) or the indicated concentrations of butaprost or CAY10684 for 24 h. *E* and *F*, cells were pretreated with vehicle, PF04418948, or ONO AE3 208 for 2 h. Subsequently, the cells were treated with vehicle, 500 nM PGE_2, or 500 nM PGE_2 plus the indicated concentrations of PF04418948 (*E*) or ONO AE3 208 (*F*) for 24 h. *C–F*, cell lysates were prepared and subjected to Western blotting. *A* and *B*, means ± S.D. (*error bars*) ($n = 6$). *, $p < 0.001$.

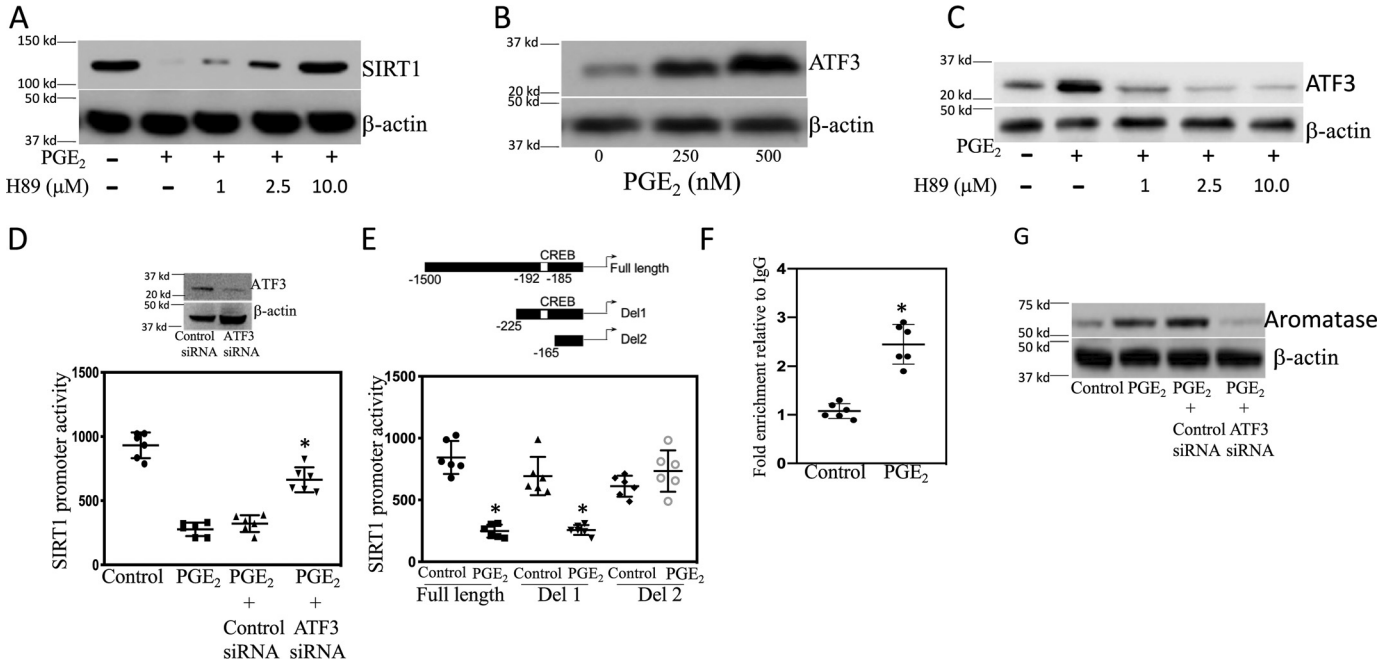

Figure 8. ATF3 is important for PGE_2-mediated down-regulation of SIRT1 in human breast ASCs. *A–G*, a human breast ASC cell line was used. *A*, cells were pretreated with vehicle or the indicated concentrations of H89, a PKA inhibitor, for 2 h and then treated with vehicle, 500 nM PGE_2, or 500 nM PGE_2 plus the indicated concentrations of H89 for 24 h. *B*, cells were treated with the indicated concentrations of PGE_2 for 2 h. Cell lysates were subjected to Western blotting, and the blots were probed as indicated. *C*, cells were pretreated with vehicle or the indicated concentrations of H89 for 2 h and then treated with vehicle, 500 nM PGE_2, or 500 nM PGE_2 plus the indicated concentrations of H89 for 24 h. *D*, cells were transfected with 0.9 μg of full-length *SIRT1* promoter and 0.2 μg of *psv*-β-gal constructs. In the *column* labeled *Control siRNA*, cells received 0.9 μg of control siRNA, and in the *column* labeled *ATF3 siRNA*, cells received 0.9 μg of ATF3 siRNA. 24 h later, cells were treated with vehicle (control) or PGE_2 for 24 h. Cells were harvested, and luciferase activity was measured. Luciferase activity was normalized to β-gal activity. *Inset*, Western blotting was performed after transfecting ASCs with control or ATF3 siRNA. *E*, the *top panel* represents different deletions of *SIRT1* promoter used. Full-length promoter and deletion 1 (*Del1*) contain a CRE site, whereas deletion 2 (*Del2*) lacks a CRE site. Cells were transfected with 1.8 μg of each of three *SIRT1* promoter-luciferase constructs and 0.2 μg of *psv*-β-gal for 24 h. Subsequently, cells were treated with vehicle (control) or 500 nM PGE_2 for 24 h. Cells were then harvested, and luciferase activity was measured. Luciferase activity was normalized to β-gal activity. *F*, ChIP assay was performed. Cells were treated with vehicle (control) or 500 nM PGE_2 for 3 h. Chromatin fragments were immunoprecipitated with antibodies against ATF3, and the *SIRT1* promoter was amplified by real-time PCR. DNA sequencing was carried out, and the PCR products were confirmed to be the *SIRT1* promoter. This promoter was not detected when normal IgG was used or when antibody was omitted from the immunoprecipitation step. *G*, cells were either untransfected or transfected as indicated with 2 μg of siRNA to GFP (control siRNA) or ATF3 siRNA. 48 h after transfection, cells were treated with vehicle (control) or 500 nM PGE_2 for 24 h. Cell lysates were subjected to Western blotting, and the blots were probed as indicated. *D–F*, means ± S.D. (*error bars*); $n = 6$. *, $p < 0.001$.

PGE_2-mediated recruitment of p300 to the *CYP19A1* promoter. Because p300 can acetylate and stabilize HIF-1α protein, the increased interaction between p300 and HIF-1α in response to PGE_2 can help to explain the observed enhanced levels of HIF-1α protein. The fact that changes in levels of acetylated HIF-1α were paralleled by levels of HIF-1α may be due, in part, to a p300-dependent mechanism.

Based on the finding that exogenous PGE_2 down-regulated SIRT1, leading, in turn, to elevated levels of aromatase, we next focused on the regulation of *SIRT1* gene expression. PGE_2 exerts its effects by binding to four G protein–coupled receptors (EP_1–EP_4) (30). Both EP_2 and EP_4 activate cAMP signaling and induce aromatase (27). Here, we showed that PGE_2 acted via EP_2 and EP_4 to down-regulate *SIRT1* transcription. Binding of PGE_2 to EP_2 and EP_4 can activate PKA. We showed that H89, a PKA inhibitor, blocked PGE_2-mediated down-regulation of SIRT1. ATF3 is a member of the ATF/CREB family of basic leucine zipper transcription factors (31). It is induced by a variety of cellular stressors and can act as a transcriptional repressor. The ability of PGE_2 to induce ATF3 was suppressed by inhibiting PKA. This finding is consistent with previous evidence that PKA can regulate the expression of ATF3 (32). The *SIRT1* promoter contains a CRE element in its 5′-UTR (33), suggesting the possibility that the suppressive effects of PGE_2 could be mediated via this site. Silencing ATF3 attenuated the ability of PGE_2 to suppress *SIRT1* promoter activity. When transient transfection studies were conducted using different *SIRT1* promoter deletion constructs, PGE_2 failed to suppress *SIRT1* promoter activity when a construct that lacked the CRE site (bp −192 to −185) was utilized. ChIP assays indicated that treatment of cells with PGE_2 caused an increase in ATF3 binding to the *SIRT1* promoter. Taken together, these findings suggest that PGE_2 via EP_2 and EP_4 activates the PKA → ATF3 pathway, resulting in reduced SIRT1 expression (Fig. 9). The decrease in SIRT1 leads, in turn, to increased acetyl–HIF-1α and enhanced transcription of *CYP19A1*, resulting in elevated levels of the estrogen synthase aromatase.

In engineered mice, reduced levels of SIRT1 in adipose tissue have been associated with macrophage influx and the development of adipose inflammation (34, 35). A similar low-grade inflammatory process was recently linked to the pathogenesis of human breast cancer (36, 37). Taken together, the observed reduction in SIRT1 in the breast tissue of obese women may be causally linked to both subclinical inflammation and elevated aromatase expression, contributing to the increased risk of hormone receptor-positive breast cancer in obese postmenopausal women. We do note, however, that other studies have focused on SIRT1 in breast cancer cells and suggested its involvement in positively regulating aromatase expression and estrogen-induced tumor growth (37, 38). It is quite possible, therefore, that activators of SIRT1 will have different effects on the risk of estrogen-dependent breast cancer, depending on whether a woman is obese or lean. Although future studies will be needed to address this question, the current study is the first to demonstrate that post-translational modification of HIF-1α is a determinant of aromatase expression. Whether other post-translational modifications that affect HIF-1α levels also modulate aromatase expression should be considered.

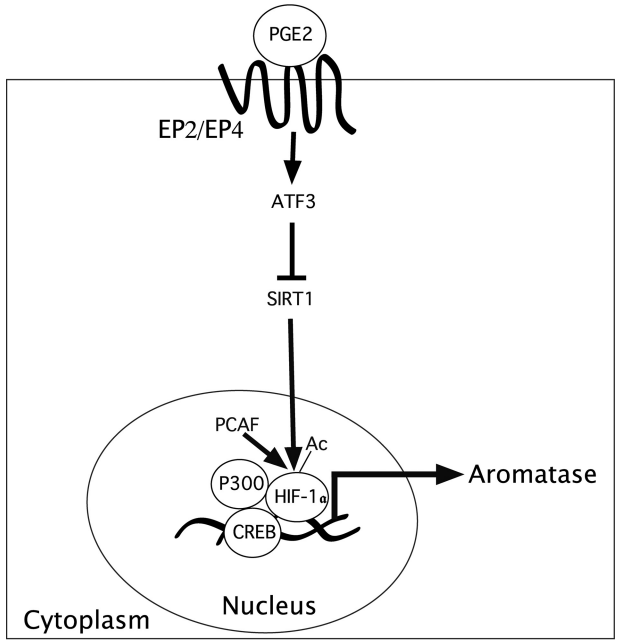

Figure 9. SIRT1 is important for PGE_2-mediated induction of aromatase expression. Obese women express lower levels of SIRT1 and higher levels of acetyl–HIF-1α, HIF-1α, and aromatase in breast tissue. PGE_2 acted via the EP_2 and EP_4 receptors to induce ATF3, a repressive transcription factor, which bound to a CRE site within the *SIRT1* promoter, resulting in reduced SIRT1 levels. The reduction in SIRT1, a deacetylase, leads to elevated levels of acetyl–HIF-1α and HIF-1α and enhanced aromatase transcription. PCAF acetylates HIF-1α and enhances its interaction with p300, a coactivator of CREB, leading to enhanced aromatase transcription. Collectively, these findings suggest the importance of SIRT1-mediated post-translational modification of HIF-1α as a determinant of the elevated levels of aromatase in the breast tissue of obese women.

Experimental procedures

Materials

Primers for aromatase, SIRT1720, and an antibody to β-actin were purchased from Sigma. Monoclonal aromatase antibody 677 was obtained from the Baylor College of Medicine (39). Antibodies to SIRT1 (1:1000; D1D7), p300 (1:1000; D8Z4E), ATF3 (1:1000; D2Y5W), and HIF-1α (1:1000; D2U3T) and microsomal isolation kits were bought from Cell Signaling Technology. Acetyllysine antibody was from Abcam (1:1000; ab80178). Control siRNA (GFP), and ATF3 and PCAF siRNAs were obtained from Thermo Fisher Scientific. Hypoxia-responsive element luciferase (HRE-luciferase), control vector, SIRT1 expression vector, and *SIRT1* promoter constructs were from GeneCopoeia. PGE_2, butaprost, PF04418948, CAY10684, resveratrol, ONO AE3208, and H89 were from Cayman. The aromatase promoter (*CYP19*PII)-luciferase construct was kindly provided by Dr. S. Chen (City of Hope, Duarte, CA).

Study population and samples

The study was approved by the institutional review boards of Weill Cornell Medical College and Memorial Sloan Kettering Cancer Center. Breast tissues used in the study were from women undergoing mastectomy at Memorial Sloan Kettering Cancer Center who were consented under a standard tissue acquisition protocol. This patient cohort has been described previously (40). Normal breast tissue from a quadrant uninvolved by tumor was collected and stored at −80 °C. BMI

was calculated from height (in meters) and weight (kg) measurements obtained before surgery. Standard definitions were used to categorize BMI as underweight or normal weight (BMI $<$ 25), overweight (BMI between 25.0 and 29.9), or obese (BMI $\geq$ 30).

Cell culture

An immortalized human mammary ASC line (HMS32-hTERT) was provided by Dr. Brittney-Shea Herbert (Indiana University School of Medicine) and grown as described previously (28, 41–43). Primary human breast ASCs and media were purchased from Zen-Bio.

Immunoprecipitation

Immunoprecipitation experiments were performed using a catch and release reversible immunoprecipitation system from Upstate Biotechnology. Cell or tissue lysate protein (500–1000 μg) was used for immunoprecipitation following the manufacturer's instructions.

Western blotting

Cells and tissues were sonicated in a lysis buffer (150 mM NaCl, 100 mM Tris, pH 8.0, 1% Tween 20, 50 mM diethyldithiocarbamate, 1 mM EDTA, 1 mM phenylmethylsulfonyl fluoride, 10 μg/ml aprotinin, 10 μg/ml trypsin inhibitor, and 10 μg/ml leupeptin). Minute adipose tissue fractionation kits were purchased from Invent Biotechnologies Inc. and used to remove lipid from tissue lysates. The protein concentration was determined according to Lowry *et al.* (44). To measure the levels of aromatase, SIRT1, acetyl–HIF-1α, and HIF-1-α proteins, tissue lysates were prepared from frozen nontumorous breast tissue samples. For aromatase, microsomal protein was isolated from tissue lysates using differential centrifugation. The microsomal suspension was subjected to immunoprecipitation with antiserum to aromatase followed by Western blotting. SIRT1 and HIF-1α proteins were immunoprecipitated, and Western blotting was performed. For acetyl–HIF-1α, immunoprecipitation was performed first with an antibody to acetyllysine, and then the blots were probed with HIF-1α antibody. β-Actin levels were assessed in whole tissue lysates by Western blotting. For the *in vitro* studies, Western blots that are representative of a minimum of three independent experiments are shown.

RNA-Seq

Total RNA was isolated from nontumorous breast samples using Qiagen's RNeasy minikit. Sequencing libraries were constructed following the Illumina TrueSeq Stranded Total RNA Library preparation protocol with rRNA depletion. Next-generation sequencing was performed with paired-end 51 bp using the Illumina HiSeq4000 platform (Weill Cornell Medicine). Raw sequenced reads were aligned to the human reference genome (hg19) using STAR (version 2.4.2) aligner. Aligned reads were quantified against the reference annotation (hg19) to obtain fragments per kilobase per million (FPKM) and raw counts using CuffLinks (version 2.2.1) and HTSeq, respectively.

Quantitative real-time PCR

Total RNA was isolated from cells using the RNeasy minikit (Qiagen) and reverse-transcribed using murine leukemia virus reverse transcriptase and oligo(dT)$_{16}$ primer. The resulting cDNA was then used for amplification. Primers for human aromatase have been described previously (11, 28, 43). The following SIRT1 primers were used: forward, 5′-CTGGACAATTCCAGCCATCT-3′; reverse, 5′-GGGTGGCAACTCTGACAAAT-3′. β-Actin (QT00095431) primers were obtained from Qiagen. β-Actin was used as an endogenous normalization control. Real-time PCR was done using 2$\times$ SYBR Green PCR master mix on a 7500 real-time PCR system (Applied Biosystems). Using the $\Delta\Delta C_T$ (relative quantification) analysis protocol, relative -fold induction was determined.

Transient transfections

50–70% confluent cultures were grown in 6-well dishes. The cells were then transfected using Lipofectamine 2000 (Invitrogen) for 24 h. Following transfection, the medium was replaced with serum-free medium for another 24 h. Luciferase and β-gal enzyme activities were measured in cellular extracts. Luciferase activity in cell lysates was normalized to β-gal enzymatic activity. 2 μg of control vector or SIRT1 expression vector were transfected into cells using Lipofectamine 2000 (Invitrogen) grown to 60–70% confluence.

RNA interference

Cells were transfected with 2 μg of siRNA oligonucleotides using DharmaFECT 4 transfection reagent according to the manufacturer's instructions.

ChIP assays

The ChIP assay was performed using the EpiTect ChIPoneday kit from SA Bioscience. Approximately 4 $\times$ 10^6 cells were cross-linked in a 1% formaldehyde solution at 37 °C for 10 min. Cross-linked cells were then lysed and sonicated to generate 200–1000-bp DNA fragments. Cell lysates were subjected to centrifugation, and the cleared supernatant was incubated with 4 μg of the antibodies at 4 °C overnight. Immune complexes were precipitated, washed, and eluted as described in the manufacturer's protocol. DNA–protein cross-links were reversed by heating at 65 °C for 4 h, and the DNA fragments were purified and used as a template for PCR amplification. Quantitative real-time PCR was carried out. For ChIP analysis, the *CYP19A1* oligonucleotide sequences for PCR primers were 5′-AACCTGATGAAGTCACAA-3′ (forward) and 5′-TCAGACATTTAGGCAAGACT-3′ (reverse). This primer set covers the *CYP19A1* promoter I.3/II segment from nucleotide −302 to −38. For ChIP analysis, the *SIRT1* oligonucleotide sequences for PCR primers were 5′-CTTCCAGCCCAGGCGGAGCG-3′ (forward) and 5′-GATTTAAACCCCATCACGTGACCCG-3′ (reverse). This primer set covers the human *SIRT1* promoter region containing the CRE site from nucleotide −225 to −21. The primers were obtained from Sigma. PCR was performed at 94 °C for 30 s, 62 °C for 30 s, and 72 °C for 45 s for 35 cycles, and real-time PCR was performed at 95 °C for 15 s and 60 °C for 60 s for 40 cycles. The PCR product generated from the ChIP template was sequenced, and the identity of the *CYP19A1* and *SIRT1* promoters was confirmed.

Statistics

Comparisons between two independent groups were made by Student's *t* test. A difference between groups of $p < 0.05$ was considered significant. For the human study, correlation between SIRT1 expression in terms of $\log_2$-transformed FPKM values and each of the continuous variables, including BMI and the relative aromatase expression, was examined using Spearman's method. Differences in SIRT1 expression across BMI categories were examined using the nonparametric Kruskall–Wallis test. Pairwise comparisons were carried out using the Wilcoxon rank sum test, and *p* values were adjusted for multiple comparisons using the Bonferroni–Holm method.

Author contributions—K. S. and A. J. D. conceptualization; K. S., N. M. I., M. M., and A. J. D. resources; K. S., N. M. I., O. E., and X. K. Z. data curation; K. S. and X. K. Z. formal analysis; K. S. validation; K. S. investigation; K. S. visualization; K. S. methodology; K. S. and A. J. D. writing-original draft; K. S. and A. J. D. project administration; K. S., N. M. I., M. M., O. E., X. K. Z., and A. J. D. writing-review and editing; A. J. D. supervision; A. J. D. funding acquisition.

References

1. Munsell, M. F., Sprague, B. L., Berry, D. A., Chisholm, G., and Trentham-Dietz, A. (2014) Body mass index and breast cancer risk according to postmenopausal estrogen-progestin use and hormone receptor status. *Epidemiol. Rev.* **36,** 114–136 CrossRef Medline
2. Rohan, T. E., Heo, M., Choi, L., Datta, M., Freudenheim, J. L., Kamensky, V., Ochs-Balcom, H. M., Qi, L., Thomson, C. A., Vitolins, M. Z., Wassertheil-Smoller, S., and Kabat, G. C. (2013) Body fat and breast cancer risk in postmenopausal women: a longitudinal study. *J. Cancer Epidemiol.* **2013,** 754815 Medline
3. Trentham-Dietz, A., Newcomb, P. A., Storer, B. E., Longnecker, M. P., Baron, J., Greenberg, E. R., and Willett, W. C. (1997) Body size and risk of breast cancer. *Am. J. Epidemiol.* **145,** 1011–1019 CrossRef Medline
4. Iyengar, N. M., Hudis, C. A., and Dannenberg, A. J. (2015) Obesity and cancer: local and systemic mechanisms. *Annu. Rev. Med.* **66,** 297–309 CrossRef Medline
5. Calle, E. E., Rodriguez, C., Walker-Thurmond, K., and Thun, M. J. (2003) Overweight, obesity, and mortality from cancer in a prospectively studied cohort of U.S. adults. *N. Engl. J. Med.* **348,** 1625–1638 CrossRef Medline
6. Ewertz, M., Jensen, M. B., Gunnarsdóttir, K. Á., Højris, I., Jakobsen, E. H., Nielsen, D., Stenbygaard, L. E., Tange, U. B., and Cold, S. (2011) Effect of obesity on prognosis after early-stage breast cancer. *J. Clin. Oncol.* **29,** 25–31 CrossRef Medline
7. Protani, M., Coory, M., and Martin, J. H. (2010) Effect of obesity on survival of women with breast cancer: systematic review and meta-analysis. *Breast Cancer Res. Treat.* **123,** 627–635 CrossRef Medline
8. Sparano, J. A., Zhao, F., Martino, S., Ligibel, J. A., Perez, E. A., Saphner, T., Wolff, A. C., Sledge, G. W., Jr., Wood, W. C., and Davidson, N. E. (2015) Long-term follow-up of the E1199 phase III trial evaluating the role of taxane and schedule in operable breast cancer. *J. Clin. Oncol.* **33,** 2353–2360 CrossRef Medline
9. Simpson, E. R., Mahendroo, M. S., Means, G. D., Kilgore, M. W., Hinshelwood, M. M., Graham-Lorence, S., Amarneh, B., Ito, Y., Fisher, C. R., Michael, M. D., Mendelson, C. R., and, Bulun, S. E. (1994) Aromatase cytochrome P450, the enzyme responsible for estrogen biosynthesis. *Endocr. Rev.* **15,** 342–355 CrossRef Medline
10. Morris, P. G., Hudis, C. A., Giri, D., Morrow, M., Falcone, D. J., Zhou, X. K., Du, B., Brogi, E., Crawford, C. B., Kopelovich, L., Subbaramaiah, K., and Dannenberg, A. J. (2011) Inflammation and increased aromatase expression occur in the breast tissue of obese women with breast cancer. *Cancer Prev. Res.* (*Phila.*) **4,** 1021–1029 CrossRef Medline
11. Subbaramaiah, K., Morris, P. G., Zhou, X. K., Morrow, M., Du, B., Giri, D., Kopelovich, L., Hudis, C. A., and Dannenberg, A. J. (2012) Increased levels of COX-2 and prostaglandin E2 contribute to elevated aromatase expression in inflamed breast tissue of obese women. *Cancer Discov.* **2,** 356–365 CrossRef Medline
12. Samarajeewa, N. U., Yang, F., Docanto, M. M., Sakurai, M., McNamara, K. M., Sasano, H., Fox, S. B., Simpson, E. R., and Brown, K. A. (2013) HIF-1α stimulates aromatase expression driven by prostaglandin E2 in breast adipose stroma. *Breast Cancer Res.* **15,** R30 CrossRef Medline
13. Morris, P. G., Zhou, X. K., Milne, G. L., Goldstein, D., Hawks, L. C., Dang, C. T., Modi, S., Fornier, M. N., Hudis, C. A., and Dannenberg, A. J. (2013) Increased levels of urinary PGE-M, a biomarker of inflammation, occur in association with obesity, aging, and lung metastases in patients with breast cancer. *Cancer Prev. Res.* (*Phila.*) **6,** 428–436 CrossRef Medline
14. Bulun, S. E., Price, T. M., Aitken, J., Mahendroo, M. S., and Simpson, E. R. (1993) A link between breast cancer and local estrogen biosynthesis suggested by quantification of breast adipose tissue aromatase cytochrome P450 transcripts using competitive polymerase chain reaction after reverse transcription. *J. Clin. Endocrinol. Metab.* **77,** 1622–1628 CrossRef Medline
15. Bulun, S. E., Sharda, G., Rink, J., Sharma, S., and Simpson, E. R. (1996) Distribution of aromatase P450 transcripts and adipose fibroblasts in the human breast. *J. Clin. Endocrinol. Metab.* **81,** 1273–1277 CrossRef Medline
16. Lin, N., and Simon, M. C. (2016) Hypoxia-inducible factors: key regulators of myeloid cells during inflammation. *J. Clin. Invest.* **126,** 3661–3671 CrossRef Medline
17. Majmundar, A. J., Wong, W. J., and Simon, M. C. (2010) Hypoxia-inducible factors and the response to hypoxic stress. *Mol. Cell* **40,** 294–309 CrossRef Medline
18. Rey, S., and Semenza, G. L. (2010) Hypoxia-inducible factor-1-dependent mechanisms of vascularization and vascular remodelling. *Cardiovasc. Res.* **86,** 236–242 CrossRef Medline
19. Rahman, S., and Islam, R. (2011) Mammalian Sirt1: insights on its biological functions. *Cell Commun. Signal.* **9,** 11 CrossRef Medline
20. Chang, H. C., and Guarente, L. (2014) SIRT1 and other sirtuins in metabolism. *Trends Endocrinol. Metab.* **25,** 138–145 CrossRef Medline
21. Liang, F., Kume, S., and Koya, D. (2009) SIRT1 and insulin resistance. *Nat. Rev. Endocrinol.* **5,** 367–373 CrossRef Medline
22. Lim, J. H., Lee, Y. M., Chun, Y. S., Chen, J., Kim, J. E., and Park, J. W. (2010) Sirtuin 1 modulates cellular responses to hypoxia by deacetylating hypoxia-inducible factor 1α. *Mol. Cell* **38,** 864–878 CrossRef Medline
23. de Kreutzenberg, S. V., Ceolotto, G., Papparella, I., Bortoluzzi, A., Semplicini, A., Dalla Man, C., Cobelli, C., Fadini, G. P., and Avogaro, A. (2010) Downregulation of the longevity-associated protein sirtuin 1 in insulin resistance and metabolic syndrome: potential biochemical mechanisms. *Diabetes* **59,** 1006–1015 CrossRef Medline
24. Kurylowicz, A., Owczarz, M., Polosak, J., Jonas, M. I., Lisik, W., Jonas, M., Chmura, A., and Puzianowska-Kuznicka, M. (2016) SIRT1 and SIRT7 expression in adipose tissues of obese and normal-weight individuals is regulated by microRNAs but not by methylation status. *Int. J. Obes.* (*Lond.*) **40,** 1635–1642 CrossRef Medline
25. Song, Y. S., Lee, S. K., Jang, Y. J., Park, H. S., Kim, J. H., Lee, Y. J., and Heo, Y. S. (2013) Association between low SIRT1 expression in visceral and subcutaneous adipose tissues and metabolic abnormalities in women with obesity and type 2 diabetes. *Diabetes Res. Clin. Pract.* **101,** 341–348 CrossRef Medline
26. Pedersen, S. B., Olholm, J., Paulsen, S. K., Bennetzen, M. F., and Richelsen, B. (2008) Low Sirt1 expression, which is upregulated by fasting, in human adipose tissue from obese women. *Int. J. Obes.* (*Lond.*) **32,** 1250–1255 CrossRef Medline
27. Subbaramaiah, K., Hudis, C., Chang, S. H., Hla, T., and Dannenberg, A. J. (2008) EP2 and EP4 receptors regulate aromatase expression in human adipocytes and breast cancer cells: evidence of a BRCA1 and p300 exchange. *J. Biol. Chem.* **283,** 3433–3444 CrossRef Medline
28. Zahid, H., Subbaramaiah, K., Iyengar, N. M., Zhou, X. K., Chen, I. C., Bhardwaj, P., Gucalp, A., Morrow, M., Hudis, C. A., Dannenberg, A. J., and Brown, K. A. (2018) Leptin regulation of the p53-HIF1α/PKM2-aromatase axis in breast adipose stromal cells: a novel mechanism for the obesity-breast cancer link. *Int. J. Obes.* (*Lond.*) **42,** 711–720 CrossRef Medline

29. Geng, H., Liu, Q., Xue, C., David, L. L., Beer, T. M., Thomas, G. V., Dai, M. S., and Qian, D. Z. (2012) HIF1α protein stability is increased by acetylation at lysine 709. *J. Biol. Chem.* **287,** 35496–35505 CrossRef Medline
30. Sugimoto, Y., and Narumiya, S. (2007) Prostaglandin E receptors. *J. Biol. Chem.* **282,** 11613–11617 CrossRef Medline
31. Thompson, M. R., Xu, D., and Williams, B. R. (2009) ATF3 transcription factor and its emerging roles in immunity and cancer. *J. Mol. Med.* **87,** 1053–1060 CrossRef Medline
32. Koivisto, E., Jurado Acosta, A., Moilanen, A. M., Tokola, H., Aro, J., Pennanen, H., Säkkinen, H., Kaikkonen, L., Ruskoaho, H., and Rysä, J. (2014) Characterization of the regulatory mechanisms of activating transcription factor 3 by hypertrophic stimuli in rat cardiomyocytes. *PLoS One* **9,** e105168 CrossRef Medline
33. Noriega, L. G., Feige, J. N., Canto, C., Yamamoto, H., Yu, J., Herman, M. A., Mataki, C., Kahn, B. B., and Auwerx, J. (2011) CREB and ChREBP oppositely regulate SIRT1 expression in response to energy availability. *EMBO Rep.* **12,** 1069–1076 CrossRef Medline
34. Gillum, M. P., Erion, D. M., and Shulman, G. I. (2011) Sirtuin-1 regulation of mammalian metabolism. *Trends Mol. Med.* **17,** 8–13 CrossRef Medline
35. Hui, X., Zhang, M., Gu, P., Li, K., Gao, Y., Wu, D., Wang, Y., and Xu, A. (2017) Adipocyte SIRT1 controls systemic insulin sensitivity by modulating macrophages in adipose tissue. *EMBO Rep.* **18,** 645–657 CrossRef Medline
36. Carter, J. M., Hoskin, T. L., Pena, M. A., Brahmbhatt, R., Winham, S. J., Frost, M. H., Stallings-Mann, M., Radisky, D. C., Knutson, K. L., Visscher, D. W., and Degnim, A. C. (2018) Macrophagic "crown-like structures" are associated with an increased risk of breast cancer in benign breast disease. *Cancer Prev. Res.* (*Phila.*) **11,** 113–119 CrossRef Medline
37. Holloway, K. R., Barbieri, A., Malyarchuk, S., Saxena, M., Nedeljkovic-Kurepa, A., Cameron Mehl, M., Wang, A., Gu, X., and Pruitt, K. (2013) SIRT1 positively regulates breast cancer associated human aromatase (CYP19A1) expression. *Mol. Endocrinol* **27,** 480–490 CrossRef Medline
38. Elangovan, S., Ramachandran, S., Venkatesan, N., Ananth, S., Gnana-Prakasam, J. P., Martin, P. M., Browning, D. D., Schoenlein, P. V., Prasad, P. D., Ganapathy, V., and Thangaraju, M. (2011) SIRT1 is essential for oncogenic signaling by estrogen/estrogen receptor α in breast cancer. *Cancer Res.* **71,** 6654–6664 CrossRef Medline
39. Sasano, H., Edwards, D. P., Anderson, T. J., Silverberg, S. G., Evans, D. B., Santen, R. J., Ramage, P., Simpson, E. R., Bhatnagar, A. S., and Miller, W. R. (2003) Validation of new aromatase monoclonal antibodies for immunohistochemistry: progress report. *J. Steroid Biochem. Mol. Biol.* **86,** 239–244 CrossRef Medline
40. Iyengar, N. M., Zhou, X. K., Gucalp, A., Morris, P. G., Howe, L. R., Giri, D. D., Morrow, M., Wang, H., Pollak, M., Jones, L. W., Hudis, C. A., and Dannenberg, A. J. (2016) Systemic correlates of white adipose tissue inflammation in early-stage breast cancer. *Clin. Cancer Res.* **22,** 2283–2289 CrossRef Medline
41. Shay, J. W., Tomlinson, G., Piatyszek, M. A., and Gollahon, L. S. (1995) Spontaneous *in vitro* immortalization of breast epithelial cells from a patient with Li-Fraumeni syndrome. *Mol. Cell. Biol.* **15,** 425–432 CrossRef Medline
42. Herbert, B. S., Chanoux, R. A., Liu, Y., Baenziger, P. H., Goswami, C. P., McClintick, J. N., Edenberg, H. J., Pennington, R. E., Lipkin, S. M., and Kopelovich, L. (2010) A molecular signature of normal breast epithelial and stromal cells from Li-Fraumeni syndrome mutation carriers. *Oncotarget* **1,** 405–422 Medline
43. Subbaramaiah, K., Brown, K. A., Zahid, H., Balmus, G., Weiss, R. S., Herbert, B. S., and Dannenberg, A. J. (2016) Hsp90 and PKM2 drive the expression of aromatase in Li-Fraumeni syndrome breast adipose stromal cells. *J. Biol. Chem.* **291,** 16011–16023 CrossRef Medline
44. Lowry, O. H., Rosebrough, N. J., Farr, A. L., and Randall, R. J. (1951) Protein measurement with the folin phenol reagent. *J. Biol. Chem.* **193,** 265–275 Medline